Interactions of Hydrophobically Modified Polyvinylamines: Adsorption Behavior at Charged Surfaces and the Formation of Polyelectrolyte Multilayers with Polyacrylic Acid

Josefin Illergård,† Lars-Erik Enarsson,† Lars Wågberg,* and Monica Ek

Department of Fibre and Polymer Technology, Royal institute of Technology, SE-100 44 Stockholm, Sweden

ABSTRACT The structure and adsorption behaviors of two types of hydrophobically modified polyvinylamines (PVAm) containing substituents of hexyl and octyl chains were compared to a native polyvinylamine sample. The conformation of dissolved polyvinylamines was studied in aqueous salt solutions using dynamic light scattering. Modified PVAm showed hydrodynamic diameters similar to native PVAm, which indicated that all PVAm polymers were present as single molecules in solution. The adsorption of the polyvinylamines, both native and hydrophobically modified, from aqueous solution onto negatively charged silica surfaces was studied in situ by reflectometry and quartz crystal microgravimetry with dissipation. Polyelectrolyte multilayers (PEM) with up to nine individual layers were formed together with poly(acrylic acid). Obtained PEM structures were rigid and showed high adsorbed amounts combined with low dissipation, with similar results for both the modified and unmodified PVAm. This suggests that electrostatics dominated the PEM formation. At lower salt concentrations, the hydrophobically modified PVAm produced multilayers with low water contents, indicating that secondary interactions induced by the hydrophobic constituents can also have a significant influence on the properties of the formed layers. The surface structure of PEMs with nine individual layers was imaged in dry state using atomic force microscopy in a dynamic mode. Modified PVAm was found to induce a different structure of the PEM at 100 mM, with larger aggregates compared to those of native PVAm. From these results, it is proposed that modified PVAm can induce aggregation within the PEM, whereas PVAm remains as single molecules in solution.

KEYWORDS: polyvinylamine • hydrophobical modification • poly(acrylic acid) • polyelectrolyte multilayers • reflectometry • quartz crystal microbalance

INTRODUCTION

Hydrophobically modified (HM) polyelectrolytes constitute a special group of charged polymers with a hydrophilic polymer backbone that carries the charge and hydrophobic chains grafted to the backbone. These polymers exhibit a combination of strong electrostatic interactions and hydrophobic interactions. The electrostatic interactions are present within each polyelectrolyte chain and between polyelectrolyte molecules, not only contributing to the solubility of the polymer in aqueous solutions but also introducing repulsion between segments of equal charge. The hydrophobic interactions of the substituents typically make the polymers self-associate in aqueous systems either via intramolecular or intermolecular association (1), provided that the electrostatic repulsion between the polymer chains is overcome by processes such as electrostatic screening. There is thus a subtle balance between electrostatic and associative interactions for systems containing hydrophobically modified polyelectrolytes. It has, for example, been shown that an increase in polymer concentration leads to a large increase in solution viscosity because of intermolecular interactions when the polymer overlap concentration is passed (2). On the other hand, there is a decrease in polymer viscosity when the ionic strength is increased, both because of a decreased electrostatic repulsion and an intramolecular association between the hydrophobic groups within the polyelectrolyte chain (3). In light of these effects, it is difficult to predict how HM polyelectrolytes will adsorb at solid surfaces, because it is difficult to determine adsorption isotherms due to the above-mentioned associative behavior. It is also quite likely that HM polyelectrolytes might associate once adsorbed at the solid−liquid interface. To the best of our knowledge, relatively few studies on such systems have been reported, for example (4−6), compared to simple polyelectrolytes.

Generally, the conformation of polyelectrolytes molecules adsorbed at the solid−liquid interface is closely related to the initial conformation of the polyelectrolytes in solution (7). The charge density of the polyelectrolyte has a strong effect on chain conformation, as the chain becomes stretched with increasing charge density. This leads to an extended, linear configuration of highly charged polyelectrolytes in solution and, for the adsorption of highly charged polyelec-

* To whom correspondence should be addressed. E-mail: wagberg@kth.se.
Received for review October 12, 2009 and accepted January 5, 2010

† These authors contributed equally.

DOI: 10.1021/am9006879

trolytes, to thin adsorbed layers with polyelectrolyte segments in train configuration (8). For hydrophobically modified polyelectrolytes, the associative behavior adds to the polyelectrolyte structure. Associating polyelectrolytes can adsorb in the form of clusters rather than individual polyelectrolyte molecules. Polyelectrolytes have been shown to adsorb in clusters at higher polyelectrolyte concentrations, because of intermolecular interactions, and ellipsometry measurements show that multilayers of these aggregates can be formed at the solid−liquid interface (5).

Adsorption of polyelectrolytes provides a versatile method for surface modification that includes hydrophobic modifications. When the adsorbing polyelectrolytes carry functional groups that should be available on the most external surface after the adsorption, it is essential to clarify how the polyelectrolytes are adsorbed. If they are adsorbed as clusters, the hydrophobic groups will not be available on the surface, at least not initially, but if they are adsorbed as single layers, these groups can have a higher availability.

A related question is how the hydrophobic modification of the polyelectrolytes will affect the formation of polyelectrolyte multilayers (PEM) at the solid−liquid interface. Polyelectrolyte multilayers, as described by Decher (9), are built from a sequence of polyelectrolyte additions, altering between polycations and polyanions in the additions. For regular polyelectrolytes, the PEM build-up is characterized by an overcompensation of the surface charge, which is maintained for each layer addition. Cochin and Laschewsky (10) showed that hydrophobically modified polyelectrolytes do form PEM on quartz plates and that the polyelectrolytes uncoil upon adsorption to the interface in salt-free solutions, producing very thin layers. At higher salt concentrations, the thickness of the layers of HM polyelectrolytes was thicker than the layers from nonmodified polyelectrolytes. It was also found that the PEM from HM polyelectrolytes show a slow rearrangement over time. Because there are few investigations of HM polyelectrolytes, it is important to clarify how the properties, i.e., to the knowledge of the authors, hydrophobic modification and charge density, will alter the formation of PEM layers. This is done by examining stepwise layer growth, layer structure, and the charge compensation mechanism.

This paper focuses on hydrophobically modified polyvinylamines (PVAm). These polymers are prepared from PVAm, which is substituted with alkyl chains. Although there are several studies on conventional PVAm (11−13), little is reported about the hydrophobically modified PVAm, and their immobilization on solid surfaces remains to be studied. The modified PVAm have shown interesting antibacterial properties (14), and a simple adsorption of these polyelectrolytes to the solid−liquid interface is an interesting alternative to more complicated grafting reactions to form a nonleaching antibacterial surface (12). In the present work, the PVAm polymers modified with hexyl and octyl groups, here denoted PVAm-C_6 and PVAm-C_8, are further examined. Westman et al. have previously shown that hydrophobically modified PVAm exhibit an antibacterial effect when immobilized on a solid membrane support (15). In that study, the modified PVAm was incorporated in a polyelectrolyte multilayer (PEM) together with poly(acrylic acid) (PAA). The antibacterial mechanism behind these polymers is, however, unresolved. Several cationic polyelectrolytes have been documented to possess antibacterial qualities, and Murata et al. (16) have proposed that there is a limiting surface charge density required to get the antibacterial effect, about 1×10^{15} charged units/ cm^2. On the other hand, the choice of the hydrophobic substituent also appears to affect the antibacterial effect (14, 17). With these aspects in mind, it is important to more closely examine the PEM formation with hydrophobically modified PVAm and PAA to test how these polymers are configured and to study the localization of cationic charges and alkyl substituents, respectively. Such data can reveal if the functional groups are free to interact with the interfacing bacteria or if they are associated within the PEM and not available to particles/bacteria in solution. The conformation and aggregation behavior of PVAm has been studied both in solution and in adsorbed layers, where PVAm has been combined with poly(acrylic acid) to form PEM.

Table 1. Hydrodynamic Diameters from Dynamic Light Scattering of PVAm Polymers. Data Corresponds to *z*-Averages Obtained with Cumulant Analysis

NaCl conc (mM)	PVAm (nm)	PVAm-C_6 (nm)	PVAm-C_8 (nm)
1	44	23	31
10	42	38	39
100	43	45	39
1000	45	36	51

RESULTS

Molecular Structure of PVAm in Aqueous Solution. All PVAm samples were readily soluble in water, and visual inspection of the dissolved PVAm samples indicated that clear solutions were obtained. Table 1 shows the hydrodynamic diameter of the different PVAms in a series of salt solutions. The DLS measurements showed that the different polymers had similar hydrodynamic diameters, around 40 ± 10 nm. This indicates that PVAm is present as single molecules in solution, especially since native PVAm showed a similar-sized hydrodynamic diameter without the hydrophobic modification. However, with size distribution analysis two different diffusion regimes were found at a low salt concentration of 1 mM NaCl. These double peaks are comparable with the fast and slow diffusion modes reported by Sedlak for polyelectrolytes in low concentration salt solutions (18). At higher salt concentrations, 10 mM NaCl and above, only the fast-mode peak was found.

Figure 1 shows a comparison of the hydrodynamic diameter of the hydrophobically modified PVAm samples, measured as a function of polymer concentration at 100 mM NaCl. The size of both polymers was found to be essentially constant, about 40 nm, up to 0.8 g/L, whereas a small decrease in size was indicated at the highest concentration, 1 g/L. Most importantly, the data do not show any increase

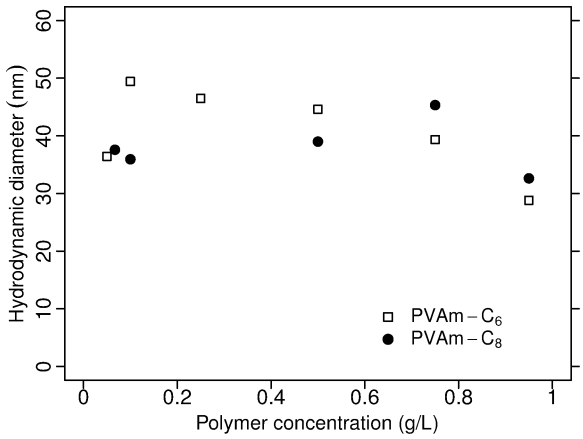

FIGURE 1. Hydrodynamic diameter of hydrophobically modified PVAm, determined with dynamic light scattering as a function of the polymer concentration.

in hydrodynamic size at increasing polymer concentrations, which suggests that no aggregation occurred in solution over the studied concentration interval.

Adsorption and Multilayer Formation of PVAm Studied with SPAR and QCM-D. Figure 2 shows the kinetics of multilayer formation of PVAm-C_6 and PAA at three different NaCl concentrations, determined with QCM-D. The Sauerbrey mass showed a stepwise layer growth (Figure 2a), supporting the formation of polyelectrolyte multilayers. Adsorption kinetics was generally fast for each layer, and the saturation plateau typically was reached within a few seconds. The pH strategy involved adsorption of PVAm at pH 7.5 and PAA at pH 3.5, because it is known that this pH combination gives high adsorption and thick layers when using weakly charged polyamines and polycarboxylic acids (19, 20).

The effect of an increasing NaCl concentration on the Sauerbrey mass was negligible between 1 and 10 mM, while it showed a clear increase at 100 mM. The corresponding dissipation data in Figure 2b were generally of small magnitudes at all the investigated salt concentrations, suggesting that the polymers adopted a flat conformation at the surface. Unlike the Sauerbrey mass, the dissipation did not strictly follow a stepwise increase with layer growth, as it appeared to stabilize on a level near 1.0×10^{-6} units after four added layers. A small fluctuation of the order of 0.1×10^{-6} units between polymer additions and rinsing was still present, as is normally observed for QCM, e.g., because of bulk viscosity effects. At 100 mM NaCl, however, there was a dynamic behavior noted for the third layer, observed as a drifting signal in both Sauerbrey mass and dissipation. This behavior was repeatable and observed for all PVAm polymers at this salt concentration.

PEM formation with different PVAm samples is further illustrated in Figure 3, comparing their adsorption at different salt concentrations. These graphs summarize the Sauerbrey mass obtained 9 min after the addition of polyelectrolytes, which represents the last minute of the rinsing step. The results correspond basically to saturation adsorption, except for the slow dynamic behavior of the second layer (PAA) at 100 mM salt, which was still drifting at the end of both the adsorption and rinsing step. An inherent variation between replicates was observed, especially for the PVAm-C_8 sample, and this is illustrated by the error bars demonstrating the standard deviation.

The corresponding plateau values in dissipation for the same QCM-D experiments is provided in the Supporting Information section. Most experiments showed a low dissipation during PEM formation, similar to the change in dissipation showed for PVAm-C_6 in Figure 2b. One clear exception was the temporary increase in dissipation at 100 mM NaCl for all PVAms in the second polyelectrolyte layer. Another exception was the gradual increase in dissipation during PEM formation that occasionally was seen for PVAm-C_8 and which therefore introduced standard deviations in the experiments.

Keeping in mind that the Sauerbrey masses include both polymer and water in the adsorbed layer, it is interesting to compare them with the reflectometer results, which provide the net polymer mass of the PEM structure. Figure 4 shows the corresponding adsorbed amounts of polymers at salt concentrations between 1 and 100 mM. The results indicated that the adsorbed mass increased nonlinearly for the first polyelectrolyte layers. After 3–5 individual layers, however, the cumulative SPAR mass unfortunately reached the upper limit of the detection limit, corresponding to approximately 18 mg/ m^2, which literally means that the PEM build-up could not be followed for as many layers as with QCM-D. Also, the SPAR data show that the adsorbed amounts increased with salt concentration. The PVAm-C_6 system showed the largest increase in PEM growth when the salt concentration was changed from 1 to 10 mM, whereas PVAm-C_8 showed the largest increase in PEM growth between 10 and 100 mM NaCl. At the highest salt concentration, the PEM growth was very similar for all polymers, with the exception that the PVAm-C_8 system deviates with a high adsorption (>18 mg/m2) after four adsorbed layers.

Surface Morphology of Polyelectrolyte Multilayers with PVAm Studied with AFM. AFM analysis of the multilayer film was performed on the dried PEM-coated quartz crystals obtained after use in adsorption experiments with QCM-D. Figure 5 shows the resulting morphology of the dry polyelectrolyte multilayers built from nine individual polyelectrolyte layers, using native PVAm, PVAm-C_6, and PVAm-C_8. At the lower salt concentration of 1 mM NaCl, the layer morphology was similar when comparing PEM built from native PVAm and PVAm-C_6 (Figure 5a) and 5c). An increase in the NaCl concentration to 100 mM affected the layer structures differently, because the PVAm-C_6 PEM showed larger, spherical aggregates (Figure 5d), whereas the native PVAm PEM revealed smaller aggregates that were joined together (Figure 5b). The corresponding surface roughness values are shown in Table 2.

Surface Contact Angles of Polyelectrolyte Multilayers with PVAm. The contact-angle analysis presented in Table 3 showed that the contact angle was higher for layers formed at 100 mM compared to 1 mM salt concentration. The hydrophobically modified polymers gave

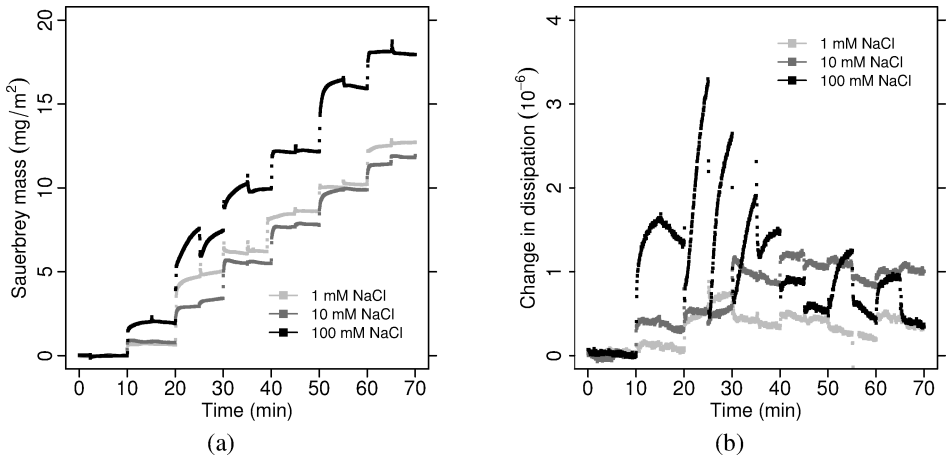

FIGURE 2. Adsorption kinetics for PVAm-C_6 at three different salt concentrations studied with the QCM-D. The layer structure changes seen in the Sauerbrey mass (a) are linked to the corresponding changes in the dissipation chart (b), as both graphs are based on the same experiments.

a higher contact angle compared to native PVAm, but multilayers based on native PVAm also rendered the surface slightly hydrophobic.

DISCUSSION

Molecular Structure of PVAm in Aqueous Solution. Analysis with dynamic light scattering (DLS) indicates that all PVAm samples were present as single molecules in solution. The critical observation for this conclusion is that the hydrophobically modified samples basically were of the same hydrodynamic size as the native PVAm. Even though the present results show double peaks in the size distribution analysis at 1 mM NaCl concentration, these appear for all samples and are therefore not unique to the hydrophobically modified samples. Because the polymers did not show aggregation at 1000 mM NaCl, it is even more unlikely that they should aggregate at 1 mM NaCl, considering the strong electrostatic repulsion that acts between the polyelectrolytes at low salt concentrations. The double peaks in DLS are instead most likely related to the polyelectrolyte character of the samples. Sedlak has shown that there is a fast and a slow diffusion mode in dynamic light scattering for polyelectrolytes at low salt concentrations, which is replaced by a single diffusion peak as the salt concentration is increased (18). It is also important to consider that the hydrophobically modified polymers might require a critical aggregation concentration to associate. The study of the hydrodynamic diameter as a function of PVAm concentration, determined in 100 mM NaCl (Figure 1), suggests that none of the hydrophobically modified PVAm samples shows any aggregation for concentrations up to 1 g/L. Thus, the studies at different background electrolyte concentrations and different polymer concentrations together indicate that PVAm is present as single molecules in solution.

Regarding the conformation of the individual PVAm molecules, all samples are polyelectrolytes with high charge densities, which has been determined previously for these samples (14). Results from DLS analysis also suggest that polyelectrolyte behavior of the polymers dominated over the associative nature in solution. Native PVAm showed hydrodynamic diameters that essentially remained constant between 1 and 1000 mM NaCl. This indicates that the polymer conformation did not change considerably by a screening electrolyte. The close distance between charged sites in PVAm is expected to give an extended conformation as the charged units repel each other. A transition toward a more coil-like structure with increasing salt concentration is typically predicted from theory for polyelectrolytes with high charge densities (21) as a result of electrostatic screening. Because the hydrodynamic size is defined from the diffusion of a spherical object, a direct physical interpretation of the size data at 1 mM NaCl should be avoided. It is more interesting to observe that a single hydrodynamic diameter around 40 nm appears at and above 10 mM NaCl, which can be related to the transition into a less extended configuration. As the molecules adopt a more uniform shape, the hydrodynamic diameter becomes a more representative measure of the molecular size.

Properties of Adsorbed Multilayers with PVAm and PAA. Adsorption data from both SPAR and QCM-D showed that the adsorbed amount per layer of PVAm increased with salt concentration. The main increase in Sauerbrey mass was obtained for the step between 10 and 100 mM NaCl. Interestingly, the effect of the hydrophobic modification on the Sauerbrey mass was very small, with the native PVAm showing a higher mass than the hydrophobically modified samples at 1 mM NaCl, whereas no differences between the samples were indicated at 100 mM NaCl for the first five layers. The adsorbed layers appear to be rigid, as the dissipation typically remained low during PEM formation. In fact, it is an exceptional result to find a dissipation rate below 2×10^{-6} with nine adsorbed polyelectrolyte layers at 100 mM, considering that the corresponding Sauerbrey mass exceeded 20 mg/m^2.

The adopted pH strategy, with PVAm adsorbed at pH 7.5 and PAA adsorbed at pH 3.5, worked generally well as the multilayers show a continuous growth and fast adsorption kinetics followed by a stable adsorption plateau (Figures 2

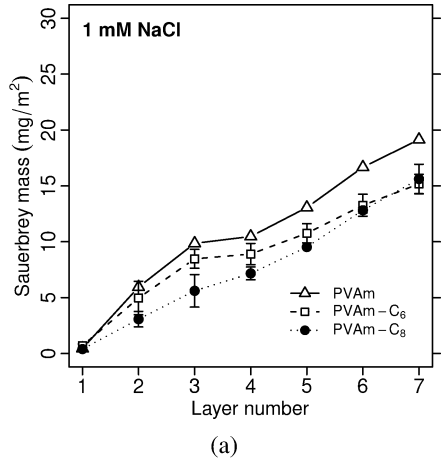

(a)

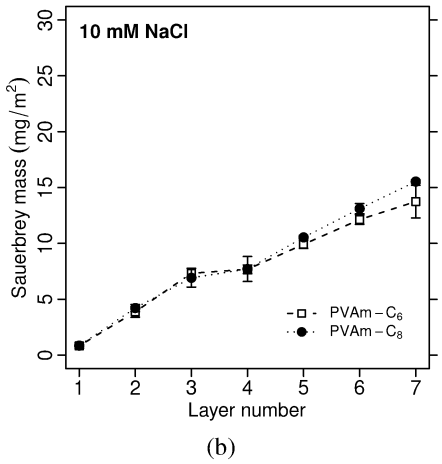

(b)

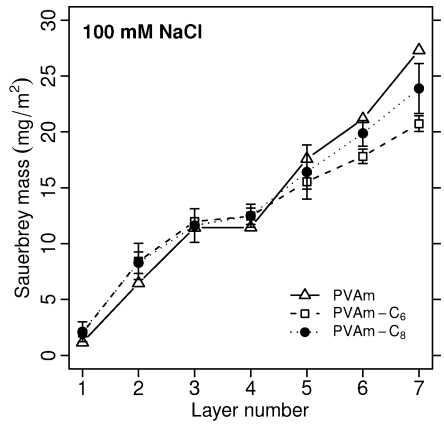

(c)

FIGURE 3. Plateau values for the Sauerbrey mass as determined with QCM-D 9 min after polymer addition. Data for NaCl concentrations of (a) 1, (b) 10, and (c) 100 mM. Error bars represent the standard deviation.

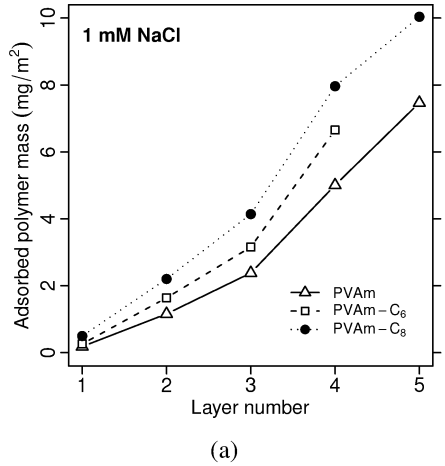

(a)

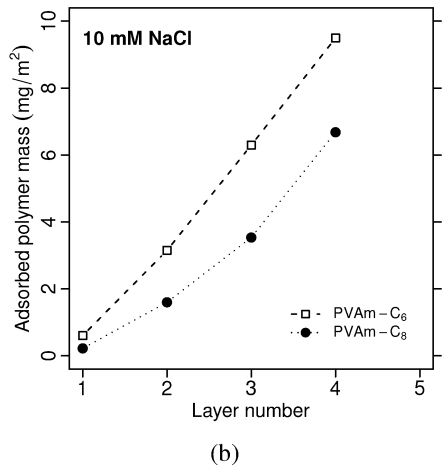

(b)

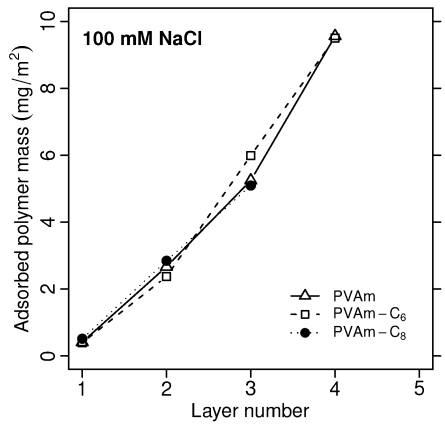

(c)

FIGURE 4. Plateau values for the cumulative adsorbed amounts of native PVAm, PVAm-C_6 and PVAm-C_8 during PEM formation with PAA. Results determined with reflectometry at salt concentrations of (a) 1, (b) 10, and (c) 100 mM.

and 3). At 100 mM NaCl, however, QCM-D revealed that adsorption of PAA in the second layer was associated with a slow dynamic mode, showing slow but continuous increases in the Sauerbrey mass and especially in the dissipation. The most intriguing effect was that the increments due to the slow dynamics were immediately lost when the salt solution was rinsed through the cell, followed by a secondary slow increase in the signals after the flow was stopped. This indicates that the effect was due to a conformational change within the PEM rather than a slow adsorption of more polyelectrolytes. A plausible explanation for the effect is sought here in the dissociation of PAA. When added as a bulk sample at pH 3.5, the PAA had a low degree of dissociation, which was intentionally utilized to improve the adsorbed mass of PAA onto PVAm. The pH within the PEM may, however, be different from the bulk value, and it is likely that an acid–base reaction took place between PVAm and PAA. The initial rapid drop in dissipation observed for the

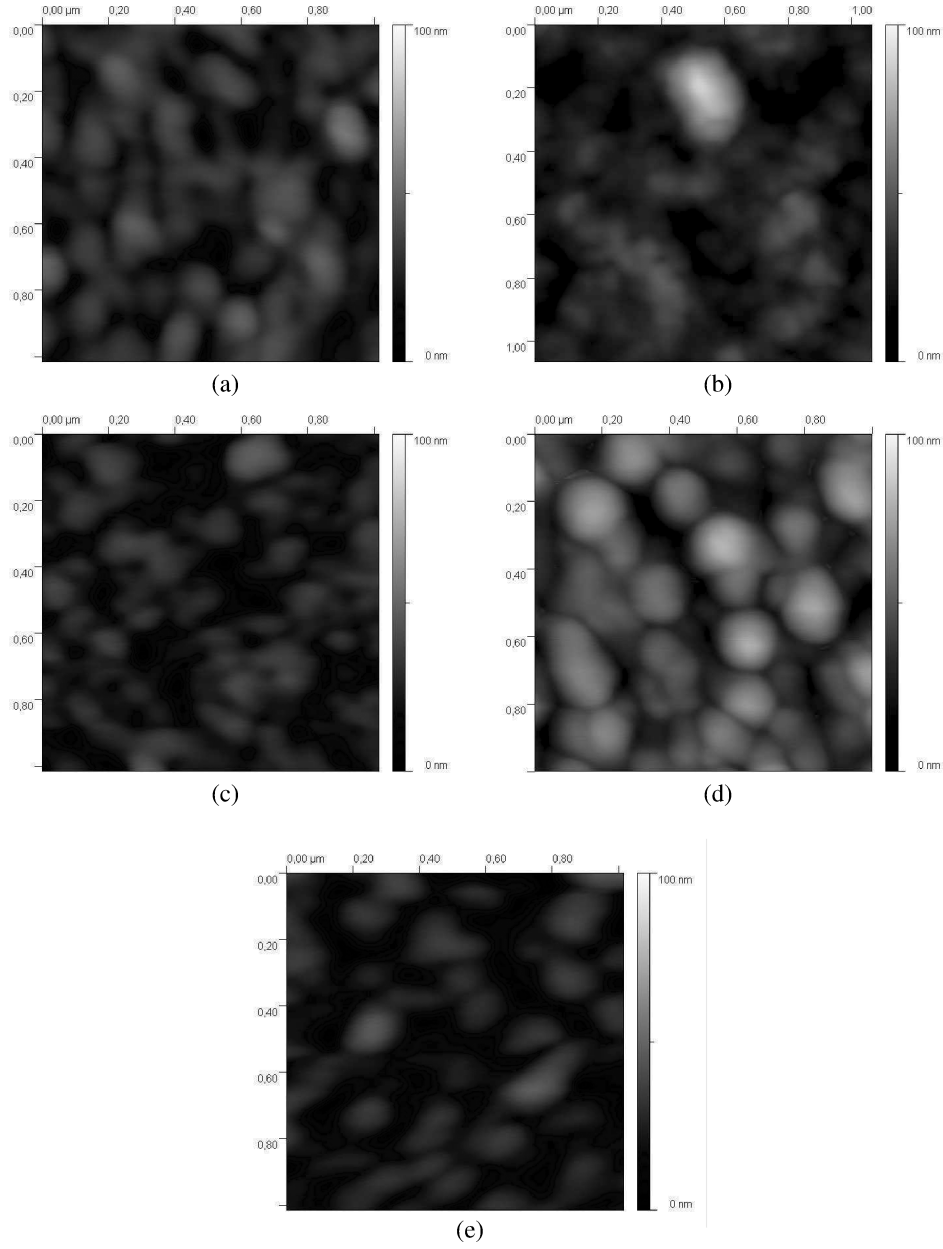

FIGURE 5. Surface morphology of multilayers of PVAm and PAA analyzed with AFM in the dynamic mode. The surfaces were treated with nine individual polyelectrolyte layers. The graphs illustrate the effect of PVAm type and background salt concentration. Native PVAm at (a) 1 and (b) 100 mM NaCl; PVAm-C_6 at (c) 1 mM NaCl and (d) 100 mM NaCl and PVAm-C_8 at (e) 100 mM NaCl.

Table 2. Surface Roughness Evaluated over Areas of $1 \times 1\ \mu m^2$, Corresponding to the AFM Images of Nine-Layer PEM Shown in Figure 5; RMS Roughness Values (R_q) and Arithmetic Averages of Absolute Values (R_a) are Listed

	R_q (nm)		R_a (nm)	
polymer	1 mM	100 mM	1 mM	100 mM
PVAm	8.0	11.8	6.4	8.6
PVAm-C_6	7.3	13.4	5.8	10.8
PVAm-C_8	N/A	7.8	N/A	6.3

Table 3. Water Contact Angles for the Multilayers in the AFM Study; Standard Deviation Is Given in Parentheses after the Contact Angle

	contact angle (deg)	
polymer	1 mM	100 mM
PVAm	55.4 (2.0)	61.2 (1.6)
PVAm-C_6	67.8 (2.1)	74.4 (0.8)
PVAm-C_8	N/A	69.0 (4.4)

second layer indicated that the first adsorbing PAA chains neutralized excess charges of immobilized PVAm. This induced a temporary compactation, but it is suggested that PAA layer later charged up and expanded. PVAm is expected to take up protons from PAA and such a reaction would introduce an excess of anionic charges in the PAA layer and consequently induce an extension and swelling of the PAA molecules. The dynamic behavior was not seen in subsequent layers, which might suggest that the acid–base balance was set after the first PAA addition onto PVAm.

SPAR data generally followed the QCM trends, but the PEM growth appeared to be nonlinear when analyzed with

SPAR, compared to the nearly linear PEM growth observed with QCM. A major difference was that SPAR detected a significant adsorption of PAA in the forth PEM layer, showing a continuous growth of PEM, whereas QCM indicated a temporary lower growth of the PEM for the fourth layer. It is here important to remember that SPAR gives the dry polymer mass and QCM gives the combined mass of polymer and trapped water in the adsorbed layer. When combined, the two methods suggest that the water content of the PEM decreased with an increasing number of adsorbed layers. This densification effect was most apparent for PAA in the forth PEM layer. The difference between the Sauerbrey mass and the SPAR mass is plotted for the PVAm samples in Figure 6 for a closer analysis. A decreasing trend in water content as a function of layer number is apparent at all the studied NaCl concentrations. The water content of the PEM was calculated to 60−80% for the first layers and decreased to 20−40% for up to five layers. The water content data should mainly be used for a relative comparison, because it is obvious that a couple of determinations provided water contents lower than zero. Both the SPAR and QCM models include a variation between replicates in the mass determination, and when the two terms are approximately equal, the difference will fluctuate around zero water content.

AFM imaging showed the dry structure of the adsorbed PEM layers (Figure 5), allowing the analysis of surface-induced structures formed during PEM formation with modified PVAm. It should be noted that removal of water alters the PEM structure, with a significant decrease in thickness. The salt concentration applied during adsorption had a strong effect on the dry topography of the PEM, as the surfaces were generally rougher at 100 mM compared to 1 mM NaCl. At the lower salt concentration, the topography of the dried PEMs showed the typical brain-pattern that is common for PEM (22). A basic feature size of about 100 nm is discernible in the AFM images of both native PVAm and PVAm-C_6 at 1 mM NaCl. It is therefore suggested that electrostatics, rather than hydrophobic interactions, determined the PEM formation at low salt concentration. The influence of hydrophobic modifications was instead observed for PEM formation at 100 mM NaCl. PEM based on native PVAm (Figure 5b) showed distinguishable features down to about 80 nm, i.e., a decrease in the smallest feature size. PEM with PVAm-C_6 (Figure 5d) showed on the other hand an increased feature size of 200 nm, indicating larger spherical aggregates. Also PVAm-C_8 showed features in the size range between 150 and 200 nm (Figure 5e). These images clearly suggest that modified PVAm formed associated structures within the PEM layer at the higher salt concentration.

It is proposed that the strong electrostatic repulsion between the PVAm molecules had to be overcome before the modified samples could associate. In solution, a screening background electrolyte was not sufficient to induce aggregation of modified PVAm molecules, as indicated by the DLS analysis. At the surface, however, the combination

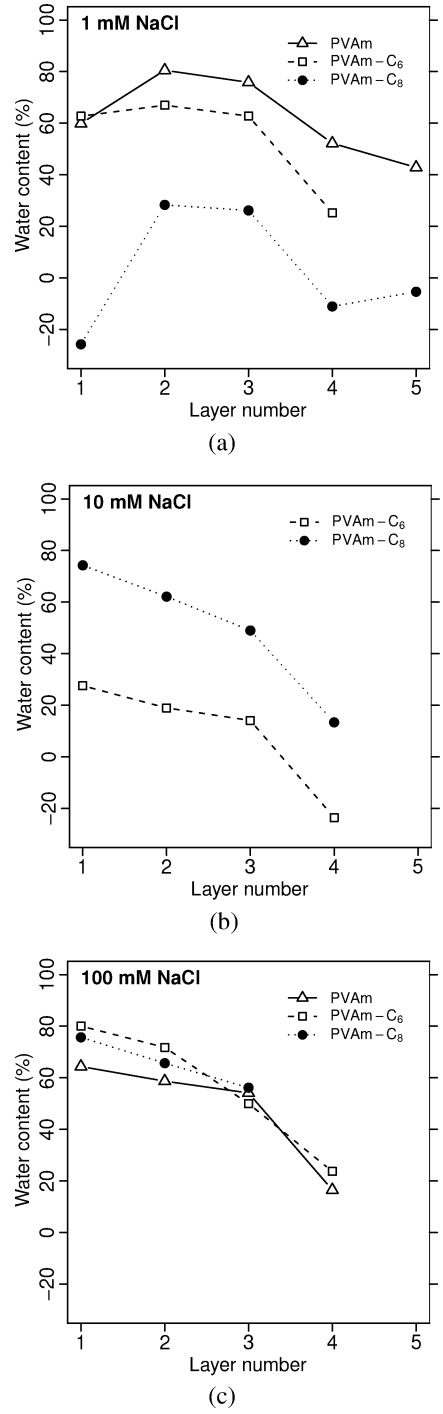

FIGURE 6. Water content of the adsorbed PEM layer calculated at salt concentrations of (a) 1, (b) 10, and (c) 100 mM.

of a screening salt and the complex formation with PAA in the PEM structure appeared to trigger the formation of larger aggregates.

Finally, it should be noted that even though the threshold for aggregation of the current modified PVAm samples appears high, it can principally be lowered either by reducing the electrostatic repulsion, e.g., lowering the charge density by reducing the degree of hydrolysis of the polyvinylformamide precursor, or by tuning the hydrophobic modification. The latter possibilities include both an increased degree of substitution and the choice of a longer alkyl chain substituent.

Table 4. Different PVAm Used in the Study[a]

polymer	substituent	degree of substitution (%)	degree of hydrolysis (%)	molecular weight (kDa)	charge density pH 7.5 (Meq/g)	charge density pH 2 (Meq/g)
PVAm			100	250	12.6	5.4
PVAm-C_6	C_6	30	90.7	340	10.4	3.2
PVAm-C_8	C_8	10	90.7	340	20.8	10.9

[a] The polymer properties are according to the suppliers specifications, except for the charge densities, that where obtained from Westman et al. (14). The charge densities at pH 7.5 were measured in presence of a phosphate buffer.

CONCLUSION

Hydrophobically modified PVAm had properties in solution similar to those of the unmodified PVAm sample. From dynamic light scattering, it was concluded that all samples were dissolved as individual polyelectrolyte chains. Thus, the polyelectrolytic nature of the polymer appeared to dominate over the hydrophobic interactions of the alkyl substituents in solution. This is probably due to the combination of high charge densities and low degrees of substitution of the hydrophobically modified PVAm samples.

The PVAm samples also showed a similar behavior in the adsorption studies by QCM-D and reflectometry. The PEMs formed on silicon oxide surfaces were flat and dense, with a low fraction of water included in the layers. Analysis of the surface topography with AFM indicated that a surface-induced aggregation of the modified PVAm occurs in the presence of a screening salt solution. Although a higher contact angle was achieved for surfaces with modified PVAm, it seems likely that the hydrophobic substituents are bound in aggregates rather than being free when using highly substituted polymers.

EXPERIMENTAL SECTION

Materials. ***Polyvinylamines.*** Tailor-made polyvinylamines (PVAm) with different degrees of modification (Table 4) were supplied by BASF. The polymers are prepared by hydrolyzing polyvinyl formamide to different degrees and thereafter grafting hydrophobic groups onto the amine groups. A more detailed description of the synthesis and chemical structure can be found elsewhere (23). The polymers were dialyzed against deionized water and thereafter freeze-dried prior to use. Charge densities of the different polymers measured by polyelectrolyte titration were obtained from Westman et al. (14).

Anionic poly(acrylic acid) (PAA) (Sigma) with an M_w of 240 000 Da according to the supplier was used without further purification. Milli-Q ultrapure water (MQ) (Millipore, Billerica, MA, US) was used to prepare all solutions.

Methods. ***DLS.*** Dynamic light scattering measurements of the polymers in solution were made with varying salt concentration and varying polymer concentration at pH 7.5. In the first case, the salt concentrations ranged from 1 mM NaCl to 1000 mM NaCl and a constant polymer concentration of 0.50 g/L was kept. For the experiments in which the polymer concentration was varied a constant NaCl concentration of 100 mM was used. Prior to analysis, the solutions were filtered through a 0.2 μm Supor syringe filter (Pall corporation, Cornwall, UK) to remove particles. The measurements were performed using a Zetasizer Nano ZS from Malvern Instruments (Malvern, UK) and the intensity peak was used to analyze the data as the z-average obtained from cumulant analysis.

QCM-D. A QCM D300 instrument (Q-Sense, Västra Frölunda, Sweden) was used for the microbalance studies. In this technique, the changes in resonance frequency of a piezoelectric crystal, Δf, is determined, which for thin and rigid films can be translated into mass using the Sauerbrey model

$$\Delta m = C\frac{\Delta f}{n} \tag{1}$$

where ΔM is the adsorbed mass, n the overtone number, and C a sensitivity factor, which depends on the type of crystal. In this study, silica-coated AT-cut quartz crystals (Q-Sense) with a C previously determined to be -0.177 mg m^{-2} Hz (24) were used. With the QCM-D technique, it is also possible to measure the energy dissipation in the adsorbed layers, and thereby get information of the rigidity of the adsorbed film. This is done by observing the decay in the resonance amplitude that occurs when the driving voltage is switched off. The dissipation factor, D, is defined as

$$D = \frac{E_{\text{dissipated}}}{2\pi E_{\text{stored}}} \tag{2}$$

where E_{stored} is the stored energy in the system and $E_{\text{dissipated}}$ is the energy dissipated during one oscillation period (25). The crystals were rinsed in a sequence of MQ−ethanol−MQ and thereafter dried under nitrogen gas. The crystals were plasma-treated for 3 min at 30 W at reduced air pressure. For the adsorption studies, polymer concentrations of 0.100 g/L were used. The NaCl concentrations tested were 1 mM, 10 mM and 100 mM. The pH was adjusted to pH 7.5 for PVAm and pH 3.5 for PAA. Rinsing solutions with the same salt concentrations and pH as the polymer solutions were prepared. To obtain a stable baseline, the instrument was run with salt solution adjusted to pH 7.5 for a minimum of 10 min. The multilayers were subsequently built up in a sequence of PVAm, rinsing at pH 7.5, PAA, and rinsing at pH 3.5. Each step lasted 5 min and was carried out at a constant temperature of 24 °C. The third overtone was used for analysis and the Sauerbrey mass was calculated.

Reflectometry. The reflectometry method has been described previously by Dijt et al. (26). In short, the output signal S is given as the intensity ratios of the parallel and perpendicular components of a polarized beam after reflection at the test surface, I_p/I_s. The adsorbed amount, Γ of a thin film is then proportional to the signal shift ΔS according to

$$\Gamma = \frac{1}{A_S}\frac{\Delta S}{S_0} \tag{3}$$

where S_0 is the initial signal and A_s is a sensitivity factor that can be calculated from a model description of the reflection coefficients from the parallel and perpendicular polarized light, R_p and R_s, according to the following equation

$$A_s = \frac{1}{R_p/R_s}\frac{d(R_p/R_s)}{d\Gamma} \quad (4)$$

Each polymer layer in the optical model is treated as a homogeneous slab described by its refractive index and thickness. After calculating the adsorbed amount for a polymer layer the refractive index of same layer was calculated according to De Feijter et al. (27).

$$n_{pol} = n_{water} + \frac{dn}{dc}\frac{\Gamma}{d} \quad (5)$$

where n_{pol} and n_{water} are refractive indices of the polymer layer and water, dn/dc is the refractive index increment, Γ is the adsorbed amount, and d is the polymer layer thickness. All polymer layer thicknesses were assumed to be 5 nm in the present optical model. This introduces apparent refractive indices, but it has been shown by Dijt et al. (26) that the calculated adsorbed amount is essentially constant as long as of the relationship between d and n is maintained according to eq 5.

Silicon wafers (Memc Electronic materials SpA, Novara, Italy) were oxidized in 1000 °C for 3 h and subsequently cut into strips. The thickness of the oxide layer was measured by null ellipsometry (type 43702−200E, Rudolph Research, Flanders NJ, USA) and was typically 80 nm. Prior to use, the strips were rinsed with a sequence of MQ−ethanol−MQ and hydrolyzed in 10% NaOH for 30 s. They were thereafter plasma treated at 10 W for 30 s at reduced air pressure. Using a stagnation point adsorption reflectometer (SPAR) (Laboratory of Physical Chemistry and Colloidal science, Wageningen University, Netherlands), the same sequence described above was used to build up the multilayers.

The adsorbed polymer mass was determined by first calculating A_S using the Prof. Huygens software (DullWare, Netherlands). By applying eq 3, we could calculate the polymer mass. The method of calculations has previously been described for two polymer layers (28) and was here extended to up to five layers. The program uses an optical model that takes the different refractive increments of the polymers into account. The refractive increments of the PVAms used in the calculations were measured with an Abbe Refractometer (Carl Zeiss, Oberkochen, Germany) and was found to be 0.23, 0.25, and 0.20 mL/g for PVAm, PVAm-C_6 and PVAm-C_8, respectively. The refractive increment for PAA, 0.147 mL/g, was obtained from Eriksson et al. (29).

The water content of the multilayers was calculated as

$$Q_{water} = \frac{m_{total} - m_{polymer}}{m_{total}} \quad (6)$$

where Q_{water} is the water content, m_{total} is the total mass of the adsorbed layer calculated from the Sauerbrey mass of QCM-D data, and $m_{polymer}$ is the polymer mass calculated from the SPAR.

AFM. Atomic force microscopy (AFM) imaging in dynamic mode using a Nanoscope III (Veeco, Santa Barbara, CA, US) was carried out on the polyelectrolyte multilayers with nine layers, which were produced on the QCM-D crystals. The crystals were dried prior the analysis. The rms surface roughness (R_q) and the arithmetic average of absolute values (R_a) were calculated using the Nanoscope software (Veeco). Standard tapping mode silicon cantilevers (RTESP) came from the same supplier.

Contact Angle Analysis. The contact angles at the water−air interface of the multilayers produced in the QCM-D instrument were analyzed with a CAM2000 (KSV, Helsinki, Finland).

Acknowledgment. The authors thank BASF SE and SCA Hygiene AB for financial support of this study. BASF SE is also acknowledged for providing the PVAm polymer samples.

Supporting Information Available: Plateau values for the change in dissipation obtained with the QCM-D experiments (PDF). This material is available free of charge via the Internet at http://pubs.acs.org.

REFERENCES AND NOTES

(1) Kötz, J.; Kosmella, S.; Beitz, T. *Prog. Polym. Sci.* **2001**, *26*, 1199–1232.
(2) Ye, L.; Mao, L.; Huang, R. *J. Appl. Polym. Sci.* **2001**, *82*, 3552–3557.
(3) Jin, W. Q.; Toutianoush, A.; Tieke, B. *Langmuir* **2003**, *19*, 2550–2553.
(4) Poncet, C.; Tiberg, F.; Audebert, R. *Langmuir* **1998**, *14*, 1697–1704.
(5) Samoshina, Y.; Nylander, T.; Claesson, P.; Schillen, K.; Iliopoulos, I.; Lindman, B. *Langmuir* **2005**, *21*, 2855–2864.
(6) Guyomard, A.; Muller, G.; Glinel, K. *Macromolecules* **2005**, *38*, 5737–5742.
(7) Falk, M.; Ödberg, L.; Wågberg, L.; Risinger, G. *Colloids Surf.* **1989**, *40*, 115–124.
(8) Fleer, G. J.; Cohen Stuart, M. A.; Scheutjens, J. M. H. M.; Cosgrove, T.; Vincent, B. *Polymers at Interfaces*, 1st ed.; Chapman and Hall: London, 1993; pp 343−375.
(9) Decher, G. *Science* **1997**, *277*, 1232–1237.
(10) Cochin, D.; Laschewsky, A. *Macromol. Chem. Phys.* **1999**, *200*, 609–615.
(11) Feng, X.; Zhang, D.; Pelton, R. *Holzforschung* **2009**, *63*, 28–32.
(12) Simon, F.; Dragan, E. S.; Bucatariu, F. *React. Funct. Polym.* **2008**, *68*, 1178–1184.
(13) Poptoshev, E.; Rutland, M. W.; Claesson, P. M. *Langmuir* **1999**, *15*, 7789–7794.
(14) Westman, E.-H.; Ek, M.; Enarsson, L.-E.; Wågberg, L. *Biomacromolecules* **2009**, *10*, 1478–1483.
(15) Westman, E.-H.; Ek, M.; Wågberg, L. *Holzforschung* **2009**, *63*, 33–39.
(16) Murata, H.; Koepsel, R. R.; Matyjaszewski, K.; Russell, A. J. *Biomaterials* **2007**, *28*, 4870–4879.
(17) Tiller, J. C.; Liao, C.-J.; Lewis, K.; Klibanov, A. M. *Proc. Natl. Acad. Sci. U.S.A.* **2001**, *98*, 5981–5985.
(18) Sedlak, M. *J. Chem. Phys.* **1996**, *105*, 10123–10133.
(19) Notley, S. M.; Eriksson, M.; Wågberg, L. *J. Colloid Interface Sci.* **2005**, *292*, 29–37.
(20) Shiratori, S. S.; Rubner, M. F. *Macromolecules* **2000**, *33*, 4213–4219.
(21) Netz, R. R.; Andelman, D. *Phys. Rep.* **2003**, *380*, 1–95.
(22) Decher, G.; Schlenoff, J. B. *Multilayer Thin Films: Sequential Assembly of Nanocomposite Materials*, 1st ed.; Wiley-VCH: Weinheim, Germany, 2003.
(23) Champ, S.; Koch, O.; Ek, M.; Westman, E.; Wågberg, L.; Feuerhake, R.; Hähnle, H. Patent WO2008055857.
(24) Edvardsson, M.; Rodahl, M.; Kasemo, B.; Hook, F. *Anal. Chem.* **2005**, *77*, 4918–4926.
(25) Rodahl, M.; Höök, F.; Krozer, A.; Brzezinski, P.; Kasemo, B. *Rev. Sci. Instrum.* **1995**, *66*, 3924–3930.
(26) Dijt, J. C.; Stuart, M. A. C.; Hofman, J. E.; Fleer, G. J. *Colloids Surf.* **1990**, *51*, 141–158.
(27) De Feijter, J. A.; Benjamins, J.; Veer, F. A. *Biopolymers* **1978**, *17*, 1759–1772.
(28) Enarsson, L.-E.; Wågberg, L. *J. Colloid Interface Sci.* **2008**, *325*, 84–92.
(29) Eriksson, M.; Notley, S. M.; Wågberg, L. *J. Colloid Interface Sci.* **2005**, *292*, 38–45.

AM9006879